Appl Microbiol Biotechnol
DOI 10.1007/s00253-016-7347-5

Genetic dissection of fruiting body-related traits using quantitative trait loci mapping in *Lentinula edodes*

Wen-bing Gong[1,2] · Lei Li[3] · Yan Zhou[1] · Yin-bing Bian[1] · Hoi-shan Kwan[3] · Man-kit Cheung[3] · Yang Xiao[1]

Received: 27 October 2015 / Revised: 18 January 2016 / Accepted: 22 January 2016

Abstract To provide a better understanding of the genetic architecture of fruiting body formation of *Lentinula edodes*, quantitative trait loci (QTLs) mapping was employed to uncover the loci underlying seven fruiting body-related traits (FBRTs). An improved *L. edodes* genetic linkage map, comprising 572 markers on 12 linkage groups with a total map length of 983.7 cM, was constructed by integrating 82 genomic sequence-based insertion-deletion (InDel) markers into a previously published map. We then detected a total of 62 QTLs for seven target traits across two segregating testcross populations, with individual QTLs contributing 5.5 %–30.2 % of the phenotypic variation. Fifty-three out of the 62 QTLs were clustered in six QTL hotspots, suggesting the existence of main genomic regions regulating the morphological characteristics of fruiting bodies in *L. edodes*. A stable QTL hotspot on MLG2, containing QTLs for all investigated traits, was identified in both testcross populations. QTLs for related traits were frequently co-located on the linkage groups, demonstrating the genetic basis for phenotypic correlation of traits. Meta-QTL (mQTL) analysis was performed and identified 16 mQTLs with refined positions and narrow confidence intervals (CIs). Nine genes, including those encoding MAP kinase, blue-light photoreceptor, riboflavin-aldehyde-forming enzyme and cyclopropane-fatty-acyl-phospholipid synthase, and cytochrome P450s, were likely to be candidate genes controlling the shape of fruiting bodies. The study has improved our understanding of the genetic architecture of fruiting body formation in *L. edodes*. To our knowledge, this is the first genome-wide QTL detection of FBRTs in *L. edodes*. The improved genetic map, InDel markers and QTL hotspot regions revealed here will assist considerably in the conduct of future genetic and breeding studies of *L. edodes*.

Keywords Shiitake mushroom · Fruiting body-related traits · QTL co-localisation · QTL hotspots · Candidate genes

Introduction

Lentinula edodes (shiitake), well known for its high nutritional and medicinal values, is one of the most cultivated, edible mushrooms worldwide, especially in East Asia. As a white-rot fungus, *L. edodes* is environmentally friendly and can convert various categories of refuse and lignocellulosic waste into food (Özçelik and Pekşen 2007).

The characteristics of fruiting bodies are crucial for shiitake's commodity value. The majority of customers tend to purchase shiitake fruiting bodies with thick and meaty caps. In a recent study, an analysis of phenotypic data derived from multiple populations suggested that fruiting body-related traits (FBRTs) of shiitake are quantitative traits controlled by multiple genes or quantitative trait loci (QTLs) (Gong et al. 2014b). Strong positive phenotypic correlations were also observed between pairs of traits associated with fruiting body formation (Gong et al. 2014b). It is difficult to improve agronomic traits with traditional breeding methods such as selection based on phenotypes. In marker-assisted selection (MAS), molecular

Electronic supplementary material The online version of this article (doi:10.1007/s00253-016-7347-5) contains supplementary material, which is available to authorized users.

✉ Yang Xiao
xiaoyang@mail.hzau.edu.cn; xyfungi@163.com

[1] Institute of Applied Mycology, Huazhong Agricultural University, Wuhan 430070, Hubei Province, People's Republic of China

[2] Institute of Bast Fiber Crops, Chinese Academy of Agricultural Sciences, Changsha 410205, People's Republic of China

[3] School of Life Sciences, The Chinese University of Hong Kong, Shatin, Hong Kong SAR, People's Republic of China

Published online: 15 February 2016

markers associated with phenotypes may be integrated into regular breeding schemes to improve the selection efficiency (Collard and Mackill 2008). The dissection of genetic architectures of quantitative traits through QTL mapping is of great value for carrying out MAS and for improving the efficiency in breeding programmes (Foulongne-Oriol 2012).

To date, QTL mapping of agronomic traits has been reported in several edible mushrooms. In *Pleurotus ostreatus*, QTLs responsible for vegetative mycelium growth rate, lignin-degrading enzymatic activities, production and quality traits have been described (Larraya et al. 2002, 2003; Santoyo et al. 2008; Sivolapova et al. 2012). In *Agaricus bisporus*, QTLs associated with cap colour, yield-related traits, resistances to diseases, the ability of fruiting at 25 °C, as well as bruising sensitivity have been detected (Moquet et al. 1999; Foulongne-Oriol et al. 2012a, b, 2014; Gao et al. 2015). In *L. edodes*, only QTLs for vegetative mycelium growth rate on different media have been reported (Miyazaki et al. 2008; Gong et al. 2014a). Although the features of fruiting bodies appear to be the main determinants of commercial value for most edible mushrooms, only a few QTLs controlling the morphological characteristics of fruiting bodies have been identified to date.

Recently, we constructed a linkage map mainly based on sequence-related amplified polymorphism (SRAP) and target region amplification polymorphism (TRAP) markers (Gong et al. 2014a). SRAP and TRAP markers are poorly informative; therefore, the practical use of this existing linkage map is limited in detecting candidate loci corresponding to important traits of interest. Here, a subset of genomic sequence-based insertion-deletion (InDel) markers was employed to improve a previous genetic map of *L. edodes*. Furthermore, combining genotypic and phenotypic data (Gong et al. 2014a, b), we performed the first genome-wide QTL analysis for FBRTs across two *L. edodes* segregating populations. The objective of our study was to detect QTLs underlying morphological traits related to fruiting body shape in *L. edodes*. Then, two integrative analyses, the identification of QTL hotspots and meta-QTL (mQTL), were performed to allow us to better understand the results of QTL mapping. Whether there are main genomic regions regulating multiple FBRTs was evaluated by detecting QTL hotspots. The meta-QTL (mQTL) analysis was also carried out to identify consensus mQTL controlling the shape of fruiting bodies in *L. edodes*. The mQTLs with refined positions and narrow confidence intervals (CIs) were employed in candidate gene discovery.

Materials and methods

Fungal strains and populations

In this study, all *L. edodes* strains, including the two monokaryon parents L205-6 and W1-26, the monokaryon population comprising 146 single-spore isolates (SSIs), and the two dikaryon testcross populations (LQ-15 and LQ-64) both comprising 146 dikaryotic strains, were described previously (Gong et al. 2014a, b). Briefly, the 146 SSIs were derived from a mature fruit body of the dikaryon generated by crossing L205-6 and W1-26, which were selected, respectively, from germinating single-spore cultures of the cultivated strains L205 (CCTCC AF 2013008) and WX1 (ACCC 50926). Then, the 146 SSIs were paired with two tester monokaryons 741-15 and 741-64, which were derived from protoclones of the wild dikaryotic strain LeQC741S (CCTCC AF 2013009), to produce dikaryon populations LQ-15 and LQ-64, respectively. The 146 SSIs in the monokaryon mapping population were used for InDel genotyping and linkage analysis. All the dikaryons in LQ-15 and LQ-64 were used for phenotype identification of agronomic traits and QTL mapping. All the tested strains were preserved in the Institute of Applied Mycology, Huazhong Agricultural University.

InDel markers development and linkage analysis

The genomes of two monokaryotic *L. edodes* strains, L205-6 and W1-26, were re-sequenced by using the Illumina next-generation sequencing (NGS) platform HiSeq2000 at Berry Genomics Co., Ltd. (Beijing, China), both with an approximate depth of 25× genome coverage. The sequencing reads of L205-6 and W1-26 were aligned to the L54A reference sequences (Kwan et al. 2012) (GenBank accession number: LOHM00000000) using the BWA software (Li and Durbin 2009) with no less than two mismatches allowed. InDels were then identified by SAMtools (Li et al. 2009). Primer 3 (Koressaar and Remm 2007) was used to design PCR primers. A total of 134 InDel primers (with insertion/deletions no less than 6 bp) were selected and used to screen for polymorphisms using DNA samples of L205-6 and W1-26 as templates. The polymorphic primers were then used in the 146 SSIs. The detailed characteristics of all InDel markers mapped in this study are provided in Table S1 in the Supplementary Material. The procedure of InDel genotyping was the same as previously described (Gong et al. 2014a).

Linkage analysis was performed using JoinMap V3.0 (Van Ooijen and Voorrips 2001), with the Kosambi function to estimate map distances (Kosambi 1943). The handling of genotype data, parameter settings of mapping, as well as visualisation of genetic map were the same as in the previous report (Gong et al. 2014a).

Phenotype identification and QTL mapping

The fruiting trials of dikaryons in LQ-15 and LQ-64 were conducted in Huazhong Agricultural University (Hubei, China, 114.35° E, 30.48° N). Phenotype screening of seven agronomic FBRTs (pileus diameter, PD; pileus thickness, PT;

pileus weight, PW; stipe length, SL; stipe diameter, SD; stipe weight SW; and the weight of a single fruiting body, WF) was reported in LQ-15 and LQ-64 populations (Gong et al. 2014b). The phenotypic data of seven FBRTs were utilised for QTL mapping here.

Based on the improved genetic linkage map, QTLs were identified by composite interval mapping (CIM) with model 6 at a walking speed of 1 cM (number of control markers = 5; window size = 10 cM) in WinQTLCart 2.5 (Zeng 1994; Wang et al. 2012). For each trait, a 1000-permutation test was performed to estimate the genome-wide logarithm of the odds (LOD) threshold for significant QTLs ($P < 0.05$). The position, additive effect, LOD-1 confidence intervals and percentage of phenotypic variation explained (PVE) were analysed to depict each QTL. For each trait, the phenotypic variation explained by all the detected QTLs (R^2 t) was determined by multiple-regression analysis as described by Foulongne-Oriol et al. (2012a). Using the software QTL IciMapping V4.0 (Li et al. 2007), the inclusive composite interval mapping (ICIM) method with mapping parameters of 1 cM step and 0.001 probabilities in stepwise regression was employed to verify the result of CIM mapping.

QTLs were denoted in the following format: the abbreviation of traits-number of linkage group (LG)-a consecutive number (e.g. *wf-II-1* represents the first QTL on MLG2 corresponding to the weight of a single fruiting body). The positions of QTLs on the genetic map were graphically exhibited using MapChart (Voorrips 2002). For the same trait, QTLs detected by CIM and ICIM were assumed to be the same loci, when their confidence intervals (CIs) overlapped and the additive values had the same sign (Foulongne-Oriol et al. 2012a). In this study, QTLs for different traits with overlapping CIs were considered to be co-located when the genetic positions of the LOD score peak of the QTLs were the same or in the overlapping regions. QTL hotspots were identified manually by searching in a sliding window of 20 cM, in which at least three adjacent or overlapping QTLs were included (Marathi et al. 2012).

Meta-QTL analysis was performed using BioMercator software v2.1 (Arcade et al. 2004). The genetic map M was chosen as the consensus map. The information (position, LOD scores, PVE, CI) of QTLs detected in LQ-15 and LQ-64 was projected onto the consensus map M. Then, meta-analysis was carried out separately for each LG. The most probable number of meta-QTL (mQTL), their position and new CIs were determined as the model which minimised the Akaike criterion (AIC). In the current study, only one InDel marker was selected from one scaffold. It was hard to establish the correspondence between cM and Mbp. An elementary approach was used to identify candidate genes. When an InDel marker was included in the CI of the mQTLs, the annotated genes close to the InDel (less than 40 kb distance) in the scaffold from which the InDel marker came (Kwan et al. 2012) were scanned to deduce putative candidate genes.

Results

Construction of an improved linkage map

Eighty-two of the 134 designed InDel markers, representing a single locus with polymorphism between L205-6 and W1-26, were integrated into the previously published map (Gong et al. 2014a) and produced an improved genetic linkage map (map M). In map M, a total of 572 markers were assigned to 12 LGs, covering a map length of 983.7 cM, with an average marker spacing of 1.8 cM (Table S2 in the Supplementary Material). The 12 LGs in map M varied in the number of markers, map length and marker density (Table S2 in the Supplementary Material). No gap larger than 20 cM was observed in map M. The mating type loci, *MAT-A* and *MAT-B*, were mapped on MLG4 and MLG9, respectively. Integrating newly developed InDels markers reduced the number of LGs (from 13 to 12) and the largest interval between two adjacent markers, as well as enhancing the marker density.

QTL mapping of seven FBRTs

Phenotypic evaluation and analysis of the seven FBRTs have been reported previously (Gong et al. 2014b). In summary, all the seven FBRTs were quantitative traits controlled by multiple genes. There were significant effects of tester monokaryons on most traits. Furthermore, significant positive correlations were observed between pairs of the seven traits relating to fruiting body shape.

QTL mapping for the seven FBRTs using CIM identified 18 and 44 QTLs in LQ-15 and LQ-64, respectively. The 62 QTLs were distributed on seven linkage groups, i.e. MLG1, MLG2, MLG4, MLG6, MLG7, MLG8 and MLG12 (Table 1, Fig. 1). The PVE of individual QTLs ranged from 5.5 to 30.2 %. The number of QTL detected for each trait in each population varied from one to eight. The total phenotypic variation explained by all QTL (R^2t) ranged from 5.6 % for SD in LQ-15 to 54.7 % for SL in LQ-64 (Table 1). Six QTLs (*pt-VI-1*, *pw-VI-1*, *sl-IV-2*, *sl-VI-3*, *sw-VII-1* and *wf-VII-2*) were identified with high PVE (over 20 %). Using ICIM, 12 and 29 QTLs for the seven FBRTs were identified in LQ-15 and LQ-64, respectively. Thirty-four QTLs were detected by both CIM and ICIM (Table 1). Only seven QTLs (one in LQ-15, six in LQ-64) were unique to ICIM (data not shown).

Pileus-related traits

In LQ-15, nine QTLs for three pileus-related traits (three for PD, two for PT and four for PW) were located on MLG1, MLG2 and MLG4 (Table 1). Three QTLs (*pd-I-1*, *pt-I-1* and *pw-I-3*) detected by both CIM and ICIM were co-located on MLG1 (130.3–132.2 cM, close to InDel marker S298-ID1 and TRAP marker mip-2-400), contributing 9.2 to 12.1 % of the

Table 1 QTLs controlling traits related to fruiting body detected in LQ-15 and LQ-64 populations

Trait	Locus	Linkage	LQ-15							LQ-64							ICIM[g]
		Group	Position (cM)[a]	Marker[b]	LOD[c]	Additive[d]	R^2 (%)	CI (cM)[e]	R^2 t (%)[f]	Position (cM)	Marker	LOD	Additive	R^2 (%)	CI (cM)	R^2 t (%)	
PD	*pd-I-1*	MLG1	131.3	mip-2-400	3.7	2.58	9.2	130.3–132.2	30.4							44.6	Y
	pd-II-1	MLG2	45.6	S48-ID1	5.5	−3.51	13.9	45.0–46.9									Y
	pd-II-2	MLG2								48.9	S306-ID1	5.9	−3.90	15.2	48.0–50.6		Y
	pd-II-3	MLG2								54.1	exg1-4-255	3.8	−3.00	9.1	53.6–55.8		
	pd-IV-1	MLG4								64.8	*MAT-A*	3.3	2.89	8.4	59.6–67.7		Y
	pd-IV-2	MLG4	96.2	S548-ID1	7.5	−3.76	19.6	95.7–100.9									Y
	pd-VI-1	MLG6								10.8	S328-ID1	4.3	−3.10	9.6	10.2–11.7		Y
	pd-VI-2	MLG6								19.3	tyr-3-380	3.0	−2.63	6.8	17.8–20.8		
	pd-VII-1	MLG7								56.0	S78-ID1	3.5	3.07	9.5	50.0–56.8		Y
	pd-XII-1	MLG12								14.4	mip-3-150	3.0	2.56	6.6	5.6–18.0		Y
					(3.1)							(3.0)					
PT	*pt-I-1*	MLG1	131.3	mip-2-400	4.4	0.85	12.1	130.3–132.3	19.5							28.0	Y
	pt-II-1	MLG2								47.9	S306-ID1	3.8	−0.79	8.6	45.0–51.0		Y
	pt-IV-1	MLG4	83.5	ME2-EM6-460	3.0	0.73	8.7	78.7–86.1									Y
	pt-VI-1	MLG6								10.2	S328-ID1	8.1	−1.32	23.7	9.9–10.8		Y
	pt-VI-2	MLG6								19.3	tyr-3-380	6.1	−1.07	15.4	18.3–19.8		
					(3.2)							(3.1)					
PW	*pw-I-1*	MLG1	122.0	ME6-EM1-280	3.2	1.92	8.7	121.1–124.5	23.2							51.5	
	pw-I-2	MLG1	131.3	mip-2-400	4.2	2.17	11.4	130.3–132.2									Y
	pw-II-1	MLG2	45.6	S48-ID1	4.7	−2.63	12.7	45.0–46.6									Y
	pw-II-2	MLG2								47.9	S306-ID1	7.1	−2.26	14.3	47.6–50.1		Y
	pw-II-3	MLG2								54.1	exg1-4-255	4.0	−1.74	8.5	53.7–55.8		
	pw-II-4	MLG2	81.3	icb-2-470	3.1	2.43	11.9	79.7–82.6									
	pw-IV-1	MLG4								66.8	*MAT-A*	3.5	1.54	6.7	61.8–66.9		Y
	pw-VI-1	MLG6								10.2	S328-ID1	8.7	−2.71	20.6	10.0–10.8		Y
	pw-VI-2	MLG6								19.3	tyr-3-380	6.2	−2.18	13.0	19.1–19.9		
	pw-VII-1	MLG7								59.0	S655-ID1	6.1	2.14	12.5	57.3–60.1		Y
	pw-VII-2	MLG7								68.0	mip-2-170	4.5	1.81	9.0	67.3–69.0		
					(3.1)							(3.2)					
SL	*sl-II-1*	MLG2	45.6	S48-ID1	4.7	−2.57	12.6	44.7–46.6	23.0							54.7	Y
	sl-II-2	MLG2								47.9	S306-ID1	7.4	−3.20	15.5	47.6–50.0		Y
	sl-II-3	MLG2								57.0	ME6-EM1-610	4.1	−2.55	9.2	56.0–57.7		
	sl-IV-1	MLG4								64.8	*MAT-A*	6.4	3.51	18.5	61.8–66.8		
	sl-IV-2	MLG4								72.7	S346-ID1	12.5	4.50	30.2	69.7–75.9		Y

Table 1 (continued)

Trait	Locus	Linkage	LQ-15							LQ-64							ICIM[g]
		Group	Position (cM)[a]	Marker[b]	LOD[c]	Additive[d]	R^2 (%)	CI (cM)[e]	R^2 t (%)[f]	Position (cM)	Marker	LOD	Additive	R^2 (%)	CI (cM)	R^2 t (%)	
	sl-IV-3	MLG4								87.1	ME6-EM3-225	8.2	3.61	20.0	86.1–87.2		
	sl-VI-1	MLG6								7.4	tyr-3-750	5.3	−2.90	13.2	6.4–8.4		Y
	sl-VI-2	MLG6								15.7	exp1-4-660	3.7	−2.38	8.6	14.7–16.8		
	sl-VII-1	MLG7								59.6	S655-ID1	2.9	1.93	5.5	56.6–60.1		Y
	sl-VIII-1	MLG8	16.0	hlh-4-220	3.7	−2.40	11.1	15.0–17.8									Y
	sl-VIII-2	MLG8	21.7	ME1-EM2-900	3.6	−2.23	9.5	20.3–23.3									
					(3.1)							(3.1)					
SD	*sd-I-1*	MLG1	113.9	ME6-EM8-210	2.5	0.69	7.4	113.7–116.7	16.5							46.6	
	sd-I-2	MLG1	122.0	ME6-EM1-280	2.6	0.70	7.5	121.2–125.7									
	sd-I-3	MLG1	131.3	mip-2-400	2.1	0.65	6.4	130.5–132.3									
	sd-II-1	MLG2								35.4	S415-ID1	3.5	−0.79	8.4	34.7–37.9		
	sd-II-2	MLG2								47.9	S306-ID1	8.6	−1.21	19.0	47.6–49.7		Y
	sd-II-3	MLG2								54.8	icb-2-260	3.2	−0.78	7.8	53.1–57		
	sd-IV-1	MLG4								71.7	S278R/F	4.5	0.92	10.9	67.5–76.6		
	sd-VI-1	MLG6								10.2	S328-ID1	4.6	−0.93	11.3	9.6–10.8		Y
	sd-VII-1	MLG7								62.0	S449-ID1	5.6	1.03	13.6	61.1–63.6		
	sd-VII-2	MLG7								68.8	ME5-EM7-340	4.1	0.83	8.7	67.3–69.5		
					(3.0)							(3.0)					
SW	*sw-II-1*	MLG2							6.0	47.9	S306-ID1	5.6	−1.00	12.8	47.5–50.5	36.6	Y
	sw-II-2	MLG2								57.0	ME6-EM1-610	2.8	−0.73	6.7	56.0–57.8		
	sw-IV-1	MLG4								71.7	S278R/F	8.2	1.29	21.3	68.4–76.7		Y
	sw-VII-1	MLG7								62.0	S449-ID1	5.4	1.08	14.2	60.8–63.5		
	sw-VIII-1	MLG8	20.8	ste3-4-380	3.0	−0.67	8.4	19.6–22.7									
					(2.8)							(2.9)					
WF	*wf-II-1*	MLG2	45.6	S48-ID1	3.3	−2.31	8.8	44.7–51.2	18.6							54.0	Y
	wf-II-2	MLG2								48.9	S306-ID1	7.4	−3.27	14.6	45.4–51.0		Y
	wf-II-3	MLG2								54.1	exg1-4-255	6.2	−2.93	11.4	53.8–56.8		
	wf-IV-1	MLG4	96.2	S548-ID1	3.6	−2.37	9.8	95.5–103.9									Y
	wf-VI-1	MLG6								10.8	S328-ID1	7.7	−3.17	14.0	10.4–11.3		Y
	wf-VI-2	MLG6								20.5	ste3-2-265	4.8	−2.62	9.3	19.5–20.8		
	wf-VII-1	MLG7								51.1	mip-4-1100	3.5	2.70	10.1	43.9–54.0		
	wf-VII-2	MLG7								59.0	S655-ID1	11.1	4.17	22.8	57.9–59.6		Y
	wf-VII-3	MLG7								68.0	mip-2-170	6.5	3.18	13.6	67.5–68.9		

Table 1 (continued)

Trait	Locus	Linkage Group	LQ-15						LQ-64						ICIM[g]
			Position (cM)[a]	Marker[b]	LOD[c]	Additive[d]	R^2 (%)	CI (cM)[e]	R^2 t (%)[f]	Position (cM)	Marker	LOD	Additive	R^2 (%)	CI (cM)	R^2 t (%)	
	wf-XII-1	MLG12			(3.1)					14.4	ME6-EM8-160	3.4 (3.1)	2.04	5.7	5.0–19.6		Y

PD pileus diameter, *PT* pileus thickness, *PW* pileus weight, *SL* stipe length, *SD* stipe diameter, *SW* stipe weight, *WF* the weight of fruiting body

[a] Position of the LOD score peak in cM

[b] Nearest marker to the LOD score peaks

[c] The significant LOD threshold based on a 1000 permutation test for each trait was indicated as the number in the brackets. For SD in LQ-15, no QTL with the LOD over the significant threshold. A minimum LOD threshold of 2.0 was chosen to declare a QTL significant

[d] The additive effect of QTLs; a minus sign means that the favourable allele of the QTL came from the parental strain W1-26, while a plus sign means that the favourable allele of the QTL came from the parental strain L205-6

[e] CI: confidence intervals supported by LOD-1

[f] R^2 t (%): total explained phenotypic variance

[g] Y indicates that the QTL was also mapped by inclusive composite interval mapping

Fig. 1 Genetic linkage map, positions of QTLs and mQTLs for fruiting body-related traits in *Lentinula edodes*. Notes: The name of each linkage group (LG) is denoted by "MLG", followed by the group number. The newly added 82 InDel markers are underlined in the genetic map. Added InDel markers showing segregation distortion are indicated with an *asterisk* ($P < 0.01$). The QTLs are shown on the right side of the LGs. The *plus* or *minus sign* following each QTL indicates that the QTL has a positive or negative additive effect, respectively. The *minus sign* means that the favourable allele of the QTL came from the parental strain W1-26, while a *plus sign* means that the favourable allele of the QTL came from the parental strain L205-6. The percentage value represents the R^2 value (percentage of explained phenotypic variation). The length of each QTL bar is represented by the LOD-1 confidence interval, the position of LOD peak is represented by a *short line* in the QTL bar. *Solid lines* represent QTLs mapped in LQ-15 and *dashed lines* for QTLs mapped in LQ-64. QTLs detected by both CIM and ICIM are indicated in *bold*. The positions and confidence intervals of mQTLs were highlighted in *red* and placed next to the initial QTLs

phenotypic variation. Furthermore, all of the three QTLs showed positive effects, and their favourable alleles were from the parental strain L205-6. Similarly, two other QTLs (*pd-II-1* and *pw-II-1*) detected by both CIM and ICIM were co-located on MLG2 (44.7–46.9 cM, linked with InDel marker S48-ID1). In LQ-64, 17 QTLs for pileus-related traits (seven for PD, three for PT and seven for PW) were located on MLG2, MLG4, MLG6, MLG7 and MLG12. Eleven of the 17 QTLs were identified by both CIM and ICIM. Nine QTLs for three pileus-related traits were co-located in three genomic regions (on MLG2, close to InDel marker S306-ID1, 47.5–51.0 cM; on MLG6, close to InDel marker S328-ID1, 9.6–11.7 cM; on MLG6, close to TRAP marker tyr-3-380, 17.8–20.8 cM) (Fig. 1), contributing 8.6 to 23.7 % of the phenotypic variation. Two QTLs *pd-II-3* and *pw-II-3* linked with TRAP marker exg1-4-255 were also co-located on LG2 (53.6–55.8 cM). The 11 QTLs in the four regions showed negative effects, indicating that their favourable alleles were from the parental strain W1-26.

Stipe-related traits

For three stipe-related traits, seven QTLs (three for SL, three for SD and one for SW) were identified in LQ-15. For SL, the QTL *sl-II-1* on MLG2 was associated with InDel marker S48-ID1 and detected by both CIM and ICIM. Two QTLs (*sl-VIII-1* and *sl-VIII-2*) were mapped on adjacent regions of MLG8. Three QTLs for SD (*sd-I-1*, *sd-I-2* and *sd-I-3*) with favourable alleles from the parental strain L205-6 were clustered on MLG1 and accounted for 16.5 % of the total phenotypic variation. Only one QTL for SW (*sw-VIII-1*) was detected on MLG8, which was co-located with *sl-VIII-2*. In LQ-64, 19 QTLs (eight for SL, seven for SD and four for SW) were identified by CIM, eight of which were also detected by ICIM. The PVEs of three QTLs (*sl-IV-2*, *sl-VI-3* and *sw-VII-1*) were over 20 %, and the major QTL *sl-IV-2* with the highest PVE (30.2 %) was close to InDel marker S346-ID1. Three QTLs (*sl-II-2*, *sd-II-2* and *sw-II-1*) for three stipe-related


MLG1
0 S502R/F
10 flp1-4-90
11 zin2-4-710
12 S72-ID1
13 S340-ID1 S32-ID1
S18-ID1
14 S446-ID1 S384-ID1
15 S260-ID1
18 chd1-2-450
19 ME4-EM3-140
20 ME3-EM2-410
21 pep1-3-160
22 ste3-2-310
23 ME4-EM3-175
24 ME4-EM3-400 ME5-EM7-360
25 ME3-EM2-350
26 ME3-EM2-300 ME7-EM8-480
27 zip1-4-1100 ME5-EM7-660
chd1-2-1100 rab-4-650
28 ste3-2-500 ftf2-3-630
man1-4-390
29 man1-4-800 cho-2-500
31 ME6-EM8-400 ME6-EM1-560
34 tel-3-720
44 exg1-4-660
45 mlg1-2-470
48 mip-3-800
51 zin2-4-900
52 ste3-3-200
53 ftf3-3-40 zin1-3-212
54 ftf3-3-380 mlg1-2-335
ME3-EM2-450 ME3-EM2-460
55 ME7-EM8-320 ME5-EM5-200
dmc1-4-450
zin2-4-100 mip-4-750
56 mlg1-2-320 ME4-EM7-260
dmc1-4-480 dmc1-4-1100
57 ME5-EM8-480 ME5-EM5-480
mdh1-4-150 dmc1-4-245
58 lup23-3-900 ME7-EM6-180
59 ME6-EM1-760 zin1-3-380
61 exg1-4-510
62 ftf3-3-600
63 exg1-4-500
65 S222-ID1
66 S26-ID1*
69 dmc1-4-175
70 ME5-EM7-600
73 eln3-4-600
74 mip-2-460
77 ME3-EM3-580
81 ftf2-3-600
82 tlg1-3-630
84 ME3-EM8-280
88 mlg1-2-310
89 ME6-EM8-75
90 ME5-EM7-620
94 icb-2-450
101 ME3-EM3-390
103 S653-ID1 S442-ID1
106 icb-2-400
108 zin2-4-480
109 ME4-EM8-430 ME6-EM8-100
110 dmc1-4-600
111 ghf30-2-175
112 mip-3-430 hlh-4-520
113 ME4-EM8-420 cut-4-500
ME6-EM8-245 ME5-EM5-260
114 ME4-EM3-380 ME6-EM8-210
115 ME1-EM4-250 cho-2-950
116 chi1-4-340
117 mdh1-4-235
118 zin2-4-380 ME5-EM8-400
119 mip-3-300 ME6-EM3-430
121 ghf30-2-370
122 ME6-EM1-280
123 ME5-EM5-460
125 chi2-3-355
126 ME3-EM5-205 chi2-3-370
127 ME7-EM5-980 ME6-EM3-240
128 ME6-EM3-600 icb-2-50
130 S298-ID1
131 mip-2-400
133 ME3-EM5-220
137 S484-ID1
pd-I-1 + 9.2%
pt-I-1 + 12.1%
pw-I-2 + 11.4%
pw-I-1 + 8.7%
sd-I-1 + 7.4%
sd-I-2 + 7.5%
mQTL-I-1
sd-I-3 + 7.5%
mQTL-I-2
MLG2
0 chi2-3-450
16 pep1-3-910
19 icb-2-335
21 exg1-4-300
22 tel-2-430
23 tel-3-470 tel-2-210
25 mip-3-230
35 S415-ID1
40 tyr-3-80
41 ME2-EM6-60 ME2-EM6-80
42 ME4-EM8-245
44 ME4-EM3-450
46 S48-ID1
47 S113-ID1
48 S306-ID1
52 gpd-4-390
53 ME5-EM7-500
54 exg1-4-255
55 icb-2-260
56 zip1-4-480
ME6-EM1-610 ME5-EM5-135
57 ME5-EM7-375
tel-4-310 ME1-EM2-240
58 mip-4-240 gb1-4-600
ME4-EM3-500 ME1-EM4-380
59 zip1-4-200
60 zin1-3-450 chi1-4-360
61 tlg1-3-320 cut-4-290
cut-4-690 ME1-EM7-240
62 zin2-4-850 pro1-4-780
63 ftf2-3-180
64 man1-4-350
65 pro1-4-800
66 ftf2-3-160
70 tel-2-480
76 ME5-EM7-480
78 eln3-4-280
80 icb-2-470
84 zip1-4-800
99 pro1-4-700
pd-II-1 - 13.9%
pd-II-2 - 15.2%
pt-II-1 - 8.6%
pd-II-3 - 9.1%
pw-II-1 - 12.7%
pw-II-2 - 14.3 %
pw-II-3 - 8.5%
pw-II-4 + 11.9%
sl-II-1 - 12.6%
sl-II-2 - 15.5%
sl-II-3 - 9.2%
sd-II-1 - 8.4%
sd-II-2 - 19.0%
sd-II-3 - 7.8%
sw-II-1 - 12.8%
sw-II-2 - 6.7%
wf-II-1 - 8.8%
wf-II-2 - 14.6%
wf-II-3 - 11.4%
mQTL-II-1
mQTL-II-2

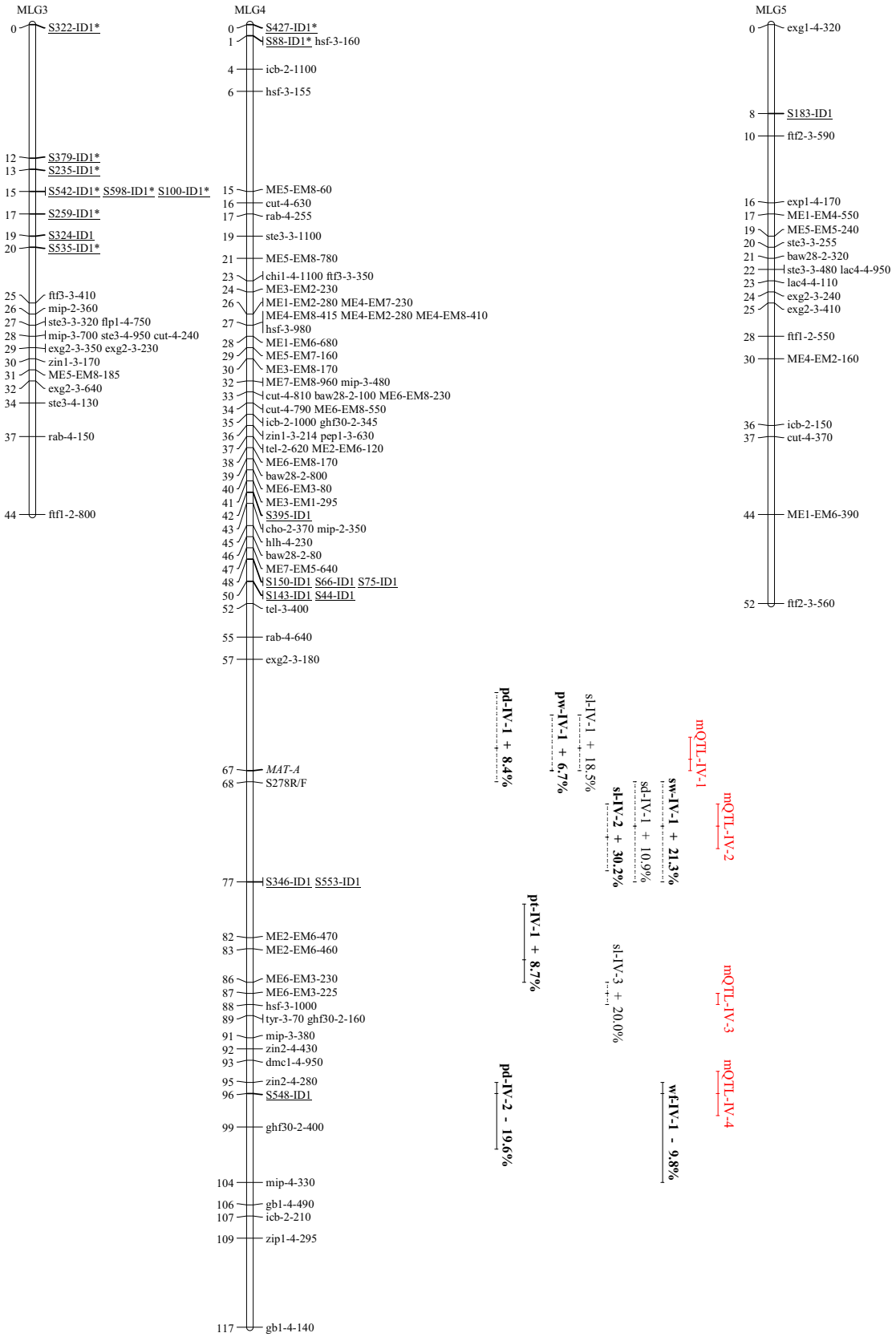

Fig. 1 (continued)

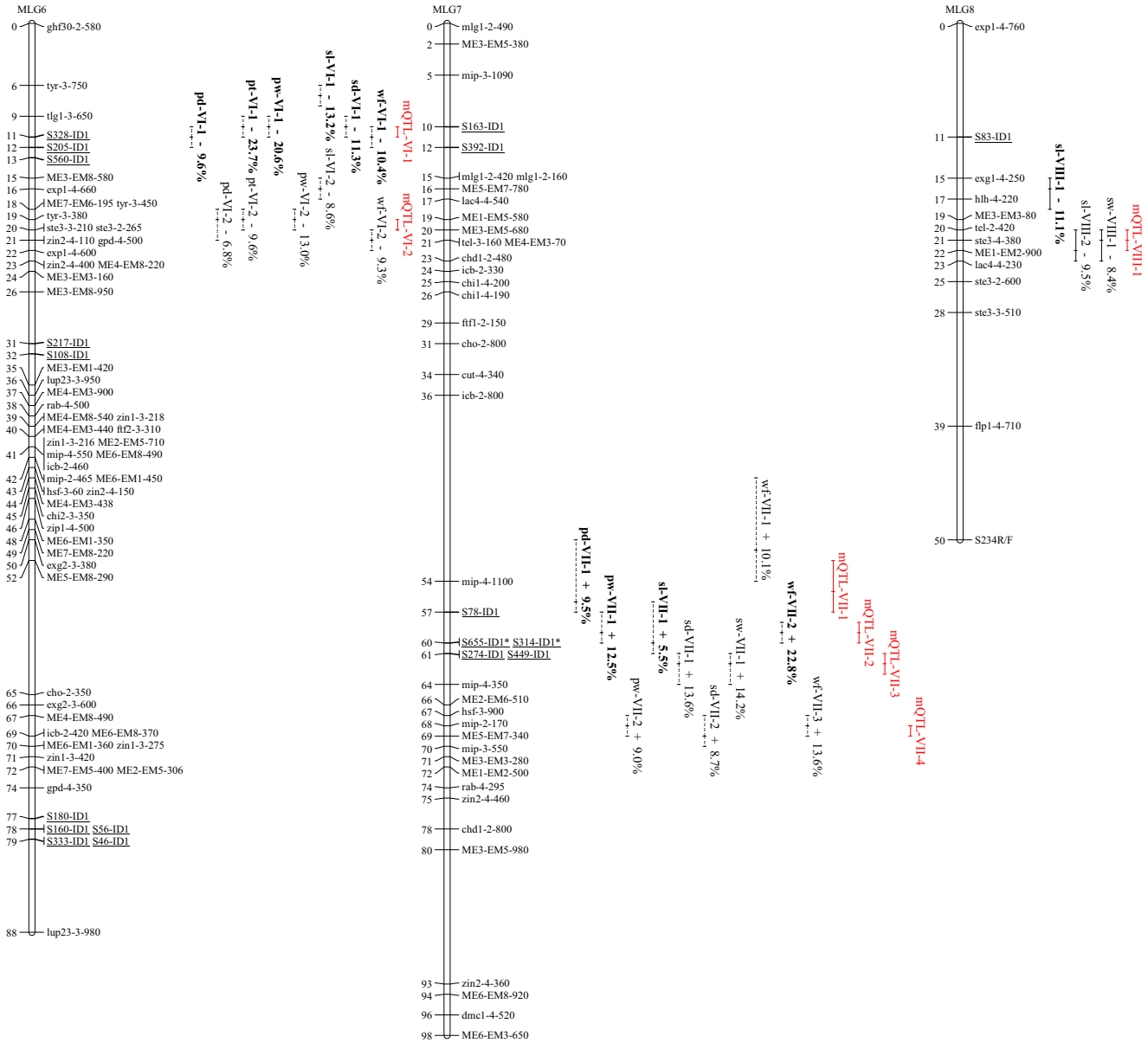

Fig. 1 (continued)

traits were co-located on the region in MLG2 adjacent to InDel marker S306-ID1.

Weight of a single fruiting body

In LQ-15, two QTLs for WF were detected by both CIM and ICIM, contributing 18.6 % of the total phenotypic variation. The QTL *wf-II-2* on MLG2 was found to be associated with InDel marker S48-ID1, while another QTL *wf-IV-1* on MLG4 was linked with InDel marker S548-ID1. Both *wf-II-2* and *wf-IV-1* showed negative effects, suggesting that the favourable alleles were contributed by W1-26. In LQ-64, eight QTLs were distributed on four LGs (MLG2, MLG6, MLG7 and MLG12), explaining 5.7 %–22.8 % of the phenotypic variation. Three QTLs (*wf-VII-1*, *wf-VII-2* and *wf-VII-3*) with favourable alleles from L205-6 were clustered on MLG7. The major QTL *wf-VII-2* was detected by both CIM and ICIM and was close to InDel marker S655-ID1. Four other QTLs (*wf-II-2*, *wf-II-3*, *wf-VI-1* and *wf-VI-2*) showed negative effects, and their favourable alleles were derived from W1-26. In the two populations, six QTLs of WF were co-located with QTLs of PW, while two QTLs of WF were co-located with QTLs of SW (Fig. 1).

QTL hotspots for FBRTs

QTL hotspots, defined as clusters containing no less than three adjacent or overlapping QTLs within a 20 cM window, were

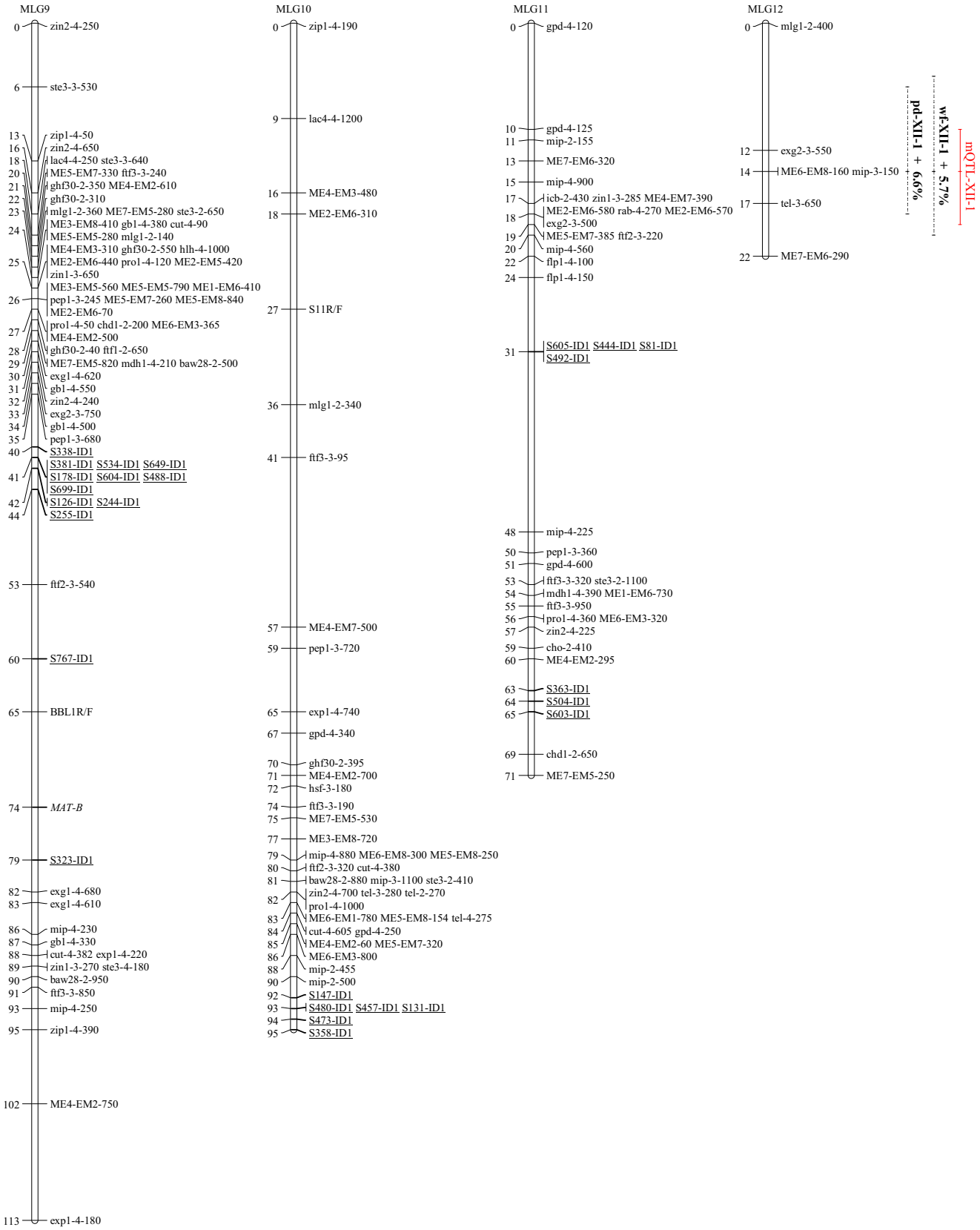

Fig. 1 (continued)

found on six LGs. Out of the 62 mapped QTLs for FBRTs, 53 (85.5 %) were clustered on MLG1, MLG2, MLG4, MLG6, MLG7 and MLG8 as QTL hotspots (Fig. 1). The most noteworthy one was the QTL hotspot on MLG2 detected in both populations. This genomic region spanned 13.1 cM (44.7–57.8 cM) and contained 17 QTLs, which were found to be involved in all the seven traits related to fruiting body of *L. edodes*. Among the 17 QTLs, four were detected in LQ-15 and 13 were detected in LQ-64. All the 17 QTLs showed negative effects, demonstrating that their favourable alleles were derived from the parental strain W1-26. Three InDel markers (S48-ID1, S113-ID1 and S306-ID1) were included in this region.

The QTL hotspot identified in LQ-64 spanned 14.4 cM (6.4–20.8 cM) on MLG6 and contained 11 QTLs mainly associated with pileus-related traits and the weight of fruiting bodies (Fig. 1). InDel markers (S328-ID1, S205-ID1 and S560-ID1) were located in this hotspot region. Another QTL hotspot detected in LQ-64 was located in the region of 50.0 to 69.5 cM on MLG7 and contained 10 QTLs for six traits. Five InDel markers (S78-ID1, S655-ID1, S314-ID1, S274-ID1 and S449-ID1) were included in this region. The hotspot region identified in LQ-64 on MLG4 (59.6–76.7 cM) contained six QTLs underlying five traits. The *MAT-A* locus and three InDel markers (S278R/F, S346-ID1 and S553-ID1) were mapped in this region. The hotspot, containing six QTLs largely specific for pileus-related traits, was detected in LQ-15 and located on MLG1 (121.1–132.3 cM). The InDel marker S298-ID1 was mapped in this region. The QTL cluster on MLG8 (15.0–23.3 cM) containing three QTLs specific for stipe-related traits was also detected in LQ-15.

Meta-QTL analysis and candidate genes

The 62 QTLs detected in the two populations were projected on the consensus map M. The meta-analysis sharply reduced the total number of QTLs from 62 to 22 mQTLs. Since meta-analysis by definition involves more than one QTL (Swamy et al. 2011), six mQTLs (two on MLG2, two on MLG6, one on MLG1 and one on MLG8) were excluded for containing only one initial QTL. In total, 16 mQTLs with two or more QTLs were considered for further analysis (Table 2). All the co-located QTLs were integrated into mQTLs. Each mQTL included 2–11 QTLs associated with 2–7 traits. The 95 % of the CIs for the mQTL varied from 0.4 to 9.4 cM, with an average of 2.6 cM. The CIs of all the 16 mQTLs were narrower than the mean of their initial QTLs. QTLs included in *mQTL-II-1* and *mQTL-IV-3* were detected in the two populations. The mQTL (*mQTL-II-1*) integrated from 11 QTLs was associated with all seven FBRTs, with all favourable alleles coming from W1-26. The CI of *mQTL-II-1* was 1.5 cM, which was half of the mean of its original QTLs (3.0 cM).

Meta-QTL with precise and narrow CI could be useful in confining the number of candidate genes. Six InDel markers (S113-ID1, S306-ID1, S548-ID1, S78-ID1, S655-ID1 and S274-ID1) were included in the CIs of five mQTLs (Table 2). Thereby, we scanned the gene contents on the six scaffolds (Le_N7_S113, Le_N7_S306, Le_N7_S548 Le_N7_S78, Le_N7_S655 and Le_N7_S274) in L54A reference genome. The physical distance per unit of recombination for *L. edodes* was roughly estimated to be 40 kb/cM in our map (40.2 Mb/983.7 cM). All the CIs of the five mQTL were over 1.0 cM. In addition to the genes containing the six InDel markers, the genes close to these markers (e.g. less than 40 kb distance) might be associated with the phenotypes. In this study, several genes (such as genes encoding MAP kinase, blue-light photoreceptor, riboflavin-aldehyde-forming enzyme and cyclopropane-fatty-acyl-phospholipid synthase and cytochrome P450s), which had been reported to be possibly involved in initiation of fruiting body formation and morphogenesis of Agaricales (see Discussion), were found to be located regions close to mQTLs. (Table S3 in the Supplementary Material).

Discussion

Improving the morphological characteristics of fruiting bodies is the long-term goal in *L. edodes* production and marketing. However, owing to the complex nature of these traits, their genetic manipulation remains challenging. In the present study, we established a more robust genetic map of *L. edodes* by integrating 82 sequence-based InDel markers into a previously published map. Then, QTL mapping for seven FBRTs traits was performed across two segregating populations. The dissection of fruiting body-related traits through QTL analysis will provide comprehensive insights into the genetic architecture of fruiting body formation and be of great use in future genetic and breeding studies of *L. edodes*.

QTLs in edible mushrooms

Like crops, many important traits in edible mushrooms are controlled by polygenic inheritance (Foulongne-Oriol 2012). Compared to other crops, research on QTL mapping in edible mushrooms is still at the initial stage. So far, a few QTLs for several agronomic traits (such as yield and disease resistance) have been identified in *P. ostreatus* and *A. bisporus* (Foulongne-Oriol 2012). However, only one trait (the weight of fruiting body) related to morphological characteristics of fruiting bodies was investigated in the two species. The QTL analysis for morphological characteristics of fruiting bodies in edible mushrooms remains to be improved. Here, we mapped

Table 2 Meta-analysis of QTLs for fruiting body-related traits

Consensus QTL	Linkage group	Position (cM)	CI (cM)	Length (cM)	Left marker	Right marker	Included InDel markers[a]	Additive effect [b]	Traits	QTL integrated
mQTL-I-1	MLG1	122.0	120.6–123.4	2.8	ME6-EM3-430	chi2–3-355	NA	+	PW, SD	*pw-I-1*, *sd-I-2*
mQTL-I-2	MLG1	131.3	130.8–131.8	1.0	S298-ID1	ME3-EM5-220	NA	+	PD, PT, PW, SD	*pd-I-1*, *pt.-I-1*, *pw-I-2*, *sd-I-3*
mQTL-II-1	MLG2	46.8	46.4–47.9	1.5	S48-ID1	gpd-4-390	S113-ID1, S306-ID1	−	PD, PT, PW,	*pd-II-1*, *pw-II-1*, *sl-II-1*, *wf-II-1*
									SL, SD, SW, WF	*pd-II-2*, *pt.-II-1*, *pw-II-2*, *sl-II-2*, *sd-II-2*, *sw-II-1*, *wf-II-2*
mQTL-II-2	MLG2	55.6	55.2–56.1	0.9	icb-2-260	ME6-EM1-610	NA	−	PD, PW, SD, SL, SW WF	*pd-II-2*, *pw-II-3*, *sd-II-3*, *sl-II-3*, *sw-II-2*, *wf-II-3*
mQTL-IV-1	MLG4	65.6	64.0–67.3	3.3	exg2-3-180	S278R/F	NA	+	PD, PW, SL	*pd-IV-1*, *pw-IV-1*, *sl-IV-1*
mQTL-IV-2	MLG4	72.2	70.0–74.4	4.4	S278R/F	S346-ID1	NA	+	SL, SD, SW	*sl-IV-2*, *sd-IV-1*, *sw-IV-1*
mQTL-IV-3	MLG4	87.0	86.5–87.6	1.1	ME6-EM3-230	hsf-3-1000	NA	+	SL, PT	*pt-IV-1*, *sl-IV-3*
mQTL-IV-4	MLG4	96.2	94.0–98.4	4.4	dmc1-4-950	ghf30-2-400	S548-ID1	−	WF, PD	*pd-IV-2*, *wf-IV-1*
mQTL-VI-1	MLG6	10.4	10.2–10.6	0.4	tlg1-3-650	S328-ID1	NA	−	PD, PT, PW, SD, WF	*pd-VI-1*, *pt.-VI-1*, *pw-VI-1*, *sd-VI-1*, *wf-VI-1*
mQTL-VI-2	MLG6	19.6	19.3–19.9	0.6	tyr-3-380	ste3-3-210	NA	−	PD, PT, PW,WF	*pd-VI-2*, *pt.-VI-2*, *pw-VI-2*, *wf-VI-2*
mQTL-VII-1	MLG7	54.5	51.7–57.3	5.6	icb-2-800	S655-ID1	S78-ID1	+	PD,WF	*wf-VII-1*, *pd.-VII-1*
mQTL-VII-2	MLG7	59.1	58.4–59.8	1.4	S78-ID1	S314-ID1	S655-ID1	+	PW, WF, SL	*pw-VII-1*, *wf-VII-2*, *sl-VII-1*
mQTL-VII-3	MLG7	62.0	61.1–62.9	1.8	S314-ID1	mip-4-350	S274-ID1	+	SD, SW	*sd-VII-1*, *sw-VII-1*
mQTL-VII-4	MLG7	68.2	67.7–68.6	0.9	hsf-3-900	ME5-EM7-340	NA	+	PW, SD, WF	*pw-VII-2*, *sd-VII-2*, *wf-VII-3*
mQTL-VIII-1	MLG8	21.3	20.2–22.3	2.1	tel-2-420	ME1-EM2-900	NA	−	SL, SW	*sl-VIII-2*, *sw-VIII-1*
mQTL-XII-1	MLG12	14.4	9.7–19.1	9.4	mlg1-2-400	ME7-EM6-290	NA	+	PD, WF	*pd-XII-1*, *wf-XII-1*

PD pileus diameter, *PT* pileus thickness, *PW* pileus weight, *SL* stipe length, *SD* stipe diameter, *SW* stipe weight, *WF* the weight of fruiting body

[a] NA indicate no InDel markers were included in the confidence intervals (CIs)

[b] The additive effect of QTLs; a minus sign means that the favourable allele of the QTL came from the parental strain W1-26, while a plus sign means that the favourable allele of the QTL came from the parental strain L205-6

QTLs for seven traits (three pileus-related traits, three stipe-related traits and the weight of a single fruiting body) associated with morphological characteristics of fruiting bodies in *L. edodes*. The weight of a single fruiting body could be divided into two parts, the weight of the pileus and of the stipe. This study provided an insight into the understanding of fruiting body composition of *L. edodes*. More QTLs of PW were found to be co-located with QTLs of WF than that of SW, suggesting that PW might account for a larger share of WF.

Effect of tester monokaryons on QTL mapping

In this study, the 146 SSIs were mated with two compatible monokaryons to produce two dikaryon populations. The QTLs detected in LQ-15 were mainly mapped on MLG1, MLG2 and MLG8, whereas most of the QTL detected in LQ-64 were located on MLG2, MLG4, MLG6 and MLG7. QTLs detected in LQ-15 and LQ-64 showed inconsistency in location, indicating strong effects of the two compatible tester strains on FBRTs. Actually, the significant effects of tester monokaryons on phenotypic data of the six FBRTs traits (except PD) were observed by the paired *t* tests (Gong et al. 2014b). The significant effects of genotype by tester lines were also reported previously (Larraya et al. 2002; Gong et al. 2014a; Foulongne-Oriol et al. 2012a, b; Gao et al. 2015).

For most edible mushrooms, heterokaryotic or dikaryotic strains are indispensable for forming fruiting bodies, from which phenotypic data of important agronomic traits (such as FBRTs) are surveyed in QTL mapping. To restore the heterokaryotic or dikaryotic phase, the SSIs are mated with compatible testers (monokaryons or homokaryons). For each locus, these mushrooms have the same allele from the tester line in one nucleus and contain either the allele from parent 1 or parent 2 in the other nucleus (Gao et al. 2015). The identified QTLs reflect the allelic substitution effect of the segregating allele with their interactions with the constant allele from the tester nucleus. The use of different segregating populations and different tester lines allowed the study of traits in different genetic backgrounds which, indeed, had great impact on the phenotype and this influenced the magnitude of QTL and, to some extent, the location (Gao et al. 2015). The differences of allelic substitution effect from tester monokaryons were also revealed by the inconsistencies in QTL detection in LQ-15 and LQ-64.

QTL hotspots for FBRTs

In the present study, QTLs for the seven FBRTs were not randomly distributed in the genome. Most of them were actually identified and concentrated in hotspot regions. This distribution pattern of QTLs provided evidence for the existence of main genomic regions regulating the morphological characteristics of fruiting bodies in *L. edodes*. It is common for the presence of QTL hotspots, often for correlated traits in plant genetic studies (Rae et al. 2009; Liu et al. 2014; Varshney et al. 2014). The existence of QTL clusters for agronomic traits was also reported in other edible mushrooms. In *P. ostreatus*, a QTL hotspot was found in linkage group VII and contained nine QTLs involved in the control of productivity traits (Larraya et al. 2003). In *A. bisporus*, a number of QTLs associated with yield-related components and resistance-related traits were clustered in QTL hotspots (Foulongne-Oriol et al. 2012a, b).

The existence of hotspots pertaining to multiple desirable traits would be beneficial to breeders (Said et al. 2013). QTL hotspots could serve as useful targets for molecular breeding as introgression of the QTL clusters could improve multiple traits simultaneously and be of great use in downstream breeding. As the hotspot on MLG2 containing a cluster of QTLs governing multiple fruiting body-related traits was identified in both LQ-15 and LQ-64 populations, it could be considered as a promising genomic region for molecular breeding. The pileus is the main edible part of *L. edodes*, and its shape has attracted great public attention (Gong et al. 2014b). Breeding programmes focused on the shape of the pileus could focus on the QTL hotspot on MLG6, which was mainly associated with pileus-related traits. Genetic manipulation on this region may be more effective for the genetic improvement of the pileus. The markers within these hotspot regions could be used as candidates in MAS.

Meta-analysis of QTLs

Meta-analysis of QTLs is an approach to integrate the information of QTLs for the same trait or related ones detected in independent studies and provides narrow confidence intervals for meta-QTLs, permitting easier positional candidate gene identification (Goffinet and Gerber 2000; Arcade et al. 2004; Khowaja et al. 2009). Examples of meta-QTL analysis were wildly used in plants (Li et al. 2011; Said et al. 2013; Costa 2015), but absent in edible mushrooms. In this study, the seven traits are closely related to each other and all control the shape of fruiting bodies in *L. edodes*. In other words, they could reflect the shape of fruiting bodies from different aspects. The integration of QTLs detected in the two dikaryon populations through meta-analysis could be an efficient and rapid approach to identify consensus mQTL and candidate genes underlying the shape of fruiting bodies in *L. edodes.*

With the limitation of mapping resolution, mapped QTL regions may harbour large CI with many markers and genes included. Candidate genes can be identified through positional cloning using QTL confidence intervals, but confidence

intervals need to be as small as possible (Semagn et al. 2013). In general, the confidence intervals of the mQTLs were narrower than their respective original QTLs (Swamy et al. 2011). In this study, the CIs of all the 16 mQTLs were narrower than the mean of their initial QTLs. The smallest CI of the mQTL was 0.4 cM. No more than two InDel markers were included in the CIs of all the 16 mQTLs. These mQTLs with refined positions and narrow CIs were more accurate for screening candidate genes.

All the co-located QTLs integrated into mQTLs, which means that the co-localisations of QTLs were verified by the meta-QTL analysis. The concordance of phenotypic and QTL patterns may demonstrate a genetic basis for the phenotypic correlations in *L. edodes*. Pleiotropy is one of the main reasons for genetic correlations between traits (Mackay et al. 2009). One possible cause for genic pleiotropy is the correlation of physiological functions or hierarchical structure between traits, where a gene is responsible for a trait which leads to, or partly contributes to, another trait (Chen and Lübberstedt 2010). In *L. edodes*, genes affecting pileus or stipe weight are likely to show genic pleiotropy with the weight of a single fruiting body. Actually, co-located QTLs affecting both the weight of the pileus and a single fruiting body were found in six regions (Fig. 1). Tight linkage of genes is also a major reason for trait correlations (Chen and Lübberstedt 2010). Unfortunately, it was difficult to determine whether the co-localisation of QTLs was due to a pleiotropic gene or tightly linked genes, with the current limited genetic mapping resolution. A fine mapping would provide additional clues for the identification of pleiotropy or tightly linked genes (Foulongne-Oriol et al. 2012a). However, the co-localisation of QTLs underlining different traits may be the genetic basis for phenotypic correlation of fruiting body-related traits in *L. edodes*.

Candidate genes underlying mQTLs

L. edodes genome sequencing and the use of sequence-based InDel markers allowed us to screen putative candidate genes in mQTL regions. Several genes, which had been reported to be possibly involved in fruiting body initiation and development of Agaricales, were found to be closely located to InDel markers included in the CIs of the mQTLs. For example, two *Le.mapk* genes were closely located to the InDel marker S113-ID1 mapped in the CI of *mQTL-II-1*. Previously, Szeto et al. (2007) characterised a developmentally regulated gene, *Le.mapk*, which encodes a mitogen-activated protein kinase and might play important roles in cell differentiation and morphogenesis during gill development of *L. edodes*. A blue-light photoreceptor gene, *Le.phrA*, was also found to be close to *mQTL-II-1* (24 kb away from S306-ID1). Sano et al. (2007) isolated a blue-light photoreceptor gene, *Le.phrA*, which was found to be transcribed at all stages of the fruiting body formation, and may be involved in photomorphogenesis of *L. edodes*.

Close to *mQTL-VII-3* on MLG7, we found an *L. edodes raf* gene (39 kb away from the InDel marker S274-ID1) encoding the riboflavin-aldehyde-forming enzyme, which catalyses oxidation of the 5′-hydroxymethyl of riboflavin to the formyl group and produces aldehyde and carboxylic acid derivatives of riboflavin (Tachibana and Oka 1981). Several studies have reported that the *raf* gene is specifically or abundantly transcribed in the course of fruiting body formation and may play an important role in fruiting body development in *L. edodes* (Hirano et al. 2004; Miyazaki et al. 2005; Chum et al. 2008). It was also reported to be associated with morphogenesis of *A. bisporus* (Sreenivasaprasad et al. 2006). Another candidate gene, highly homologous to the cyclopropane-fatty-acyl-phospholipid synthase gene (*cfs*) in *Coprinopsis cinerea*, was also located in this region (20 kb away from S274-ID1). In *C. cinerea*, the *cfs* gene was reported to putatively be involved in membrane alteration, and it was essential for fruiting body initiation (Liu et al. 2006).

Cytochrome P450s belong to a superfamily of heme-containing monooxygenases, playing critical roles in fungal biology and ecology (Park et al. 2008). The potential roles of cytochrome P450 genes in fruiting body development were implied in *L. edodes* (Akiyama et al. 2002; Miyazaki et al. 2005) and *C. cinerea* (Muraguchi and Kamada 2000). In the present study, four cytochrome P450 genes were mapped regions close to mQTLs, which might be associated with the shape of fruiting bodies in *L. edodes*.

In the current study, it was difficult to align a genome sequence to the genetic map since only one InDel marker was selected from each scaffold. Therefore, it was hard to pinpoint the genetic position of the abovementioned candidate genes on the map. It needs to be emphasised that further work is required to confirm the involvement of these genes and their variants to determine the morphological characteristics of fruiting bodies. Nevertheless, these putative candidate genes could provide a clue to unravel the molecular mechanism behind the morphogenesis of fruiting bodies in *L. edodes*. Allele-specific genetic markers developed from these genes may have potential to facilitate the genetic improvement of shiitake cultivars.

The mQTL regions with small intervals could be useful in MAS. The mQTLs yielded in this study were important regions for carrying out MAS in *L. edodes*. The *mQTL-II-1* on MLG2, integrated from 11 QTLs of all seven FBRTs, was both detected in the two populations and had priority in breeding schemes. Three InDel markers (S48-ID1, S113-ID1 and S306-ID1) in this region could be used in marker-assisted introgression of the favourable alleles from W1-26 in breeding schemes.

In conclusion, we constructed an improved *L. edodes* genetic map by integrating genomic sequence-based InDel markers into a previous map. Genetic dissection of fruiting

body-related traits was then performed across two segregating populations. By QTL analysis, we detected a total of 62 QTLs for seven FBRTs. QTLs for related traits were frequently co-located on the linkage groups, demonstrating the genetic basis for phenotypic correlation of traits. Most of the mapped QTLs here were clustered in hotspot regions, demonstrating the presence of main genomic areas responsible for the FBRTs. A special cluster of QTLs governing all investigated traits related to *L. edodes* fruiting body formation was identified on MLG2. Through meta-analysis, we identified 16 mQTLs with refined positions and narrow confidence intervals, underlying the shape of fruiting bodies. The current study also found several candidate genes (e.g. genes encoding MAP kinase, blue-light photoreceptor, riboflavin-aldehyde-forming enzyme, cyclopropane-fatty-acyl-phospholipid synthase and P450 monooxygenases) in the mQTL regions. Our results would facilitate unravelling the genetic architecture of agronomic traits related to fruiting bodies in *L. edodes*. Furthermore, the InDel markers in QTL regions can be used for marker-assisted introgression of these favourable alleles.

Acknowledgments This work was supported by the National Natural Science Foundation of China (Grant No. 31372117; 31000929), the industry (agriculture), the Science and Technology Plans of Hubei Province (Grant No. 2012DBA19001) and the Fundamental Research Funds for the Central Universities of China (Grant No. 2012ZYTS041).

Compliance with ethical standards

Ethical statement This article does not contain any studies involving human participants or animals.

Conflict of interest The authors declare that they have no competing interests.

References

Akiyama R, Sato Y, Kajiwara S, Shishido K (2002) Cloning and expression of cytochrome P450 genes, belonging to a new P450 family, of the basidiomycete *Lentinula edodes*. Biosci Biotechnol Biochem 66:2183–2188

Arcade A, Labourdette A, Falque M, Mangin B, Chardon F, Charcosset A, Joets J (2004) BioMercator: integrating genetic maps and QTL towards discovery of candidate genes. Bioinformatics 20:2324–2326

Chen Y, Lübberstedt T (2010) Molecular basis of trait correlations. Trends Plant Sci 15:454–461

Chum WW, Ng KT, Shih RS, Au CH, Kwan HS (2008) Gene expression studies of the dikaryotic mycelium and primordium of *Lentinula edodes* by serial analysis of gene expression. Mycol Res 112:950–964

Collard BCY, Mackill DJ (2008) Marker-assisted selection: an approach for precision plant breeding in the twenty-first century. Philos Trans R Soc Lond Ser B Biol Sci 363:557–572

Costa F (2015) Meta QTL analysis provides a compendium of genomic loci controlling fruit quality traits in apple. Tree Genet Genomes 11:1–11

Foulongne-Oriol M (2012) Genetic linkage mapping in fungi: current state, applications, and future trends. Appl Microbiol Biotechnol 95:891–904

Foulongne-Oriol M, Rodier A, Rousseau T, Savoie JM (2012a) Quantitative trait locus mapping of yield-related components and oligogenic control of the cap color of the button mushroom, *Agaricus bisporus*. Appl Environ Microbiol 78:2422–2434

Foulongne-Oriol M, Rodier A, Savoie JM (2012b) Relationship between yield components and partial resistance to *Lecanicillium fungicola* in the button mushroom, *Agaricus bisporus*, assessed by quantitative trait locus mapping. Appl Environ Microbiol 78:2435–2442

Foulongne-Oriol M, Navarro P, Spataro C, Ferrer N, Savoie JM (2014) Deciphering the ability of *Agaricus bisporus* var. *burnettii* to produce mushrooms at high temperature (25 °C). Fungal Genet Biol 73:1–11

Gao W, Weijn A, Baars JJ, Mes JJ, Visser RG, Sonnenberg AS (2015) Quantitative trait locus mapping for bruising sensitivity and cap color of *Agaricus bisporus* (button mushrooms). Fungal Genet Biol 77:69–81

Goffinet B, Gerber S (2000) Quantitative trait loci: a meta-analysis. Genetics 155:463–473

Gong WB, Liu W, Lu YY, Bian YB, Zhou Y, Kwan HS, Cheung MK, Xiao Y (2014a) Constructing a new integrated genetic linkage map and mapping quantitative trait loci for vegetative mycelium growth rate in *Lentinula edodes*. Fungal Biol 118:295–308

Gong WB, Xu R, Xiao Y, Zhou Y, Bian YB (2014b) Phenotypic evaluation and analysis of important agronomic traits in the hybrid and natural populations of *Lentinula edodes*. Sci Hortic 179:271–276

Hirano T, Sato T, Enei H (2004) Isolation of genes specifically expressed in the fruit body of the edible basidiomycete *Lentinula edodes*. Biosci Biotechnol Biochem 68:468–472

Khowaja FS, Norton GJ, Courtois B, Price AH (2009) Improved resolution in the position of drought-related QTLs in a single mapping population of rice by meta-analysis. BMC Genomics 10:276

Koressaar T, Remm M (2007) Enhancements and modifications of primer design program Primer3. Bioinformatics 23:1289–1291

Kosambi DD (1943) The estimation of map distance from recombination values. Ann Eugen 12:172–175

Kwan HS, Au CH, Wong MC, Qin J, Kwok ISW, Chum WWY, Yip PY, Wong KS, Li L, Huang QL, Nong YW (2012) Genome sequence and genetic linkage analysis of Shiitake mushroom *Lentinula edodes*. Nature Precedings. doi:10.1038/npre.2012.6855.1

Larraya LM, Idareta E, Arana D, Ritter E, Pisabarro AG, Ramírez L (2002) Quantitative trait loci controlling vegetative growth rate in the edible basidiomycete *Pleurotus ostreatus*. Appl Environ Microbiol 68:1109–1114

Larraya LM, Alfonso M, Pisabarro AG, Ramírez L (2003) Mapping of genomic regions (quantitative trait loci) controlling production and quality in industrial cultures of the edible basidiomycete *Pleurotus ostreatus*. Appl Environ Microbiol 69:3617–3625

Li H, Durbin R (2009) Fast and accurate short read alignment with burrows–wheeler transform. Bioinformatics 25:1754–1760

Li H, Ye G, Wang J (2007) A modified algorithm for the improvement of composite interval mapping. Genetics 175:361–374

Li H, Handsaker B, Wysoker A, Fennell T, Ruan J, Homer N, Marth G, Abecasis G, Durbin R (2009) The sequence alignment/map format and SAMtools. Bioinformatics 25:2078–2079

Li JZ, Zhang ZW, Li YL, Wang QL, Zhou YG (2011) QTL consistency and meta-analysis for grain yield components in three generations in maize. Theor Appl Genet 122:771–782

Liu Y, Srivilai P, Loos S, Aebi M, Kües U (2006) An essential gene for fruiting body initiation in the basidiomycete *Coprinopsis cinerea* is

homologous to bacterial cyclopropane fatty acid synthase genes. Genetics 172:873–884

Liu G, Jia L, Lu L, Qin D, Zhang J, Guan P, Ni Z, Yao Y, Sun Q, Peng H (2014) Mapping QTLs of yield-related traits using RIL population derived from common wheat and Tibetan semi-wild wheat. Theor Appl Genet 127:2415–2432

Mackay TFC, Stone EA, Ayroles JF (2009) The genetics of quantitative traits: challenges and prospects. Nat Rev Genet 10:565–577

Marathi B, Guleria S, Mohapatra T, Parsad R, Mariappan N, Kurungara VK, Atwal SS, Prabhu KV, Singh NK, Singh AK (2012) QTL analysis of novel genomic regions associated with yield and yield related traits in new plant type based recombinant inbred lines of rice (*Oryza sativa* L.). BMC Plant Biol 12:137

Miyazaki Y, Nakamura M, Babasaki K (2005) Molecular cloning of developmentally specific genes by representational difference analysis during the fruiting body formation in the basidiomycete *Lentinula edodes*. Fungal Genet Biol 42:493–505

Miyazaki K, Huang F, Zhang B, Shiraishi S, Sakai M, Shimaya C, Shishido K (2008) Genetic map of a basidiomycete fungus, *Lentinula edodes* (shiitake mushroom), constructed by tetrad analysis. Breeding Sci 58:23–30

Moquet F, Desmerger C, Mamoun M, Ramos-Guedes-Lafargue M, Olivier JM (1999) A quantitative trait locus of *Agaricus bisporus* resistance to *Pseudomonas tolaasii* is closely linked to natural cap color. Fungal Genet Biol 28:34–42

Muraguchi H, Kamada T (2000) A mutation in the *eln2* gene encoding a cytochrome P450 of *Coprinus cinereus* affects mushroom morphogenesis. Fungal Genet Biol 29:49–59

Özçelik E, Pekşen A (2007) Hazelnut husk as a substrate for the cultivation of shiitake mushroom (*Lentinula edodes*). Bioresour Technol 98:2652–2658

Park J, Lee S, Choi J, Ahn K, Park B, Park J, Kang S, Lee YH (2008) Fungal cytochrome P450 database. BMC Genomics 9:402

Rae AM, Street NR, Robinson KM, Harris N, Taylor G (2009) Five QTL hotspots for yield in short rotation coppice bioenergy poplar: the poplar biomass loci. BMC Plant Biol 9:23

Said JI, Lin Z, Zhang X, Song M, Zhang J (2013) A comprehensive meta QTL analysis for fiber quality, yield, yield related and morphological traits, drought tolerance, and disease resistance in tetraploid cotton. BMC Genomics 14:776

Sano H, Narikiyo T, Kaneko S, Yamazaki T, Shishido K (2007) Sequence analysis and expression of a blue-light photoreceptor gene, *Le.phrA* from the basidiomycetous mushroom *Lentinula edodes*. Biosci Biotechnol Biochem 71:2206–2213

Santoyo F, González AE, Terrón MC, Ramírez L, Pisabarro AG (2008) Quantitative linkage mapping of lignin-degrading enzymatic activities in *Pleurotus ostreatus*. Enzyme Microb Tech 43:137–143

Semagn K, Beyene Y, Warburton ML, Tarekegne A, Mugo S, Meisel B, Sehabiague P, Prasanna BM (2013) Meta-analyses of QTL for grain yield and anthesis silking interval in 18 maize populations evaluated under water-stressed and well-watered environments. BMC Genomics 14:313

Sivolapova AB, Shnyreva AV, Sonnenberg A, Baars I (2012) DNA marking of some quantitative trait loci in the cultivated edible mushroom *Pleurotus ostreatus* (Fr.) Kumm. Russ J Genet 48:383–389

Sreenivasaprasad S, Eastwood DC, Browning N, Lewis SM, Burton KS (2006) Differential expression of a putative riboflavin-aldehyde-forming enzyme (*raf*) gene during development and post-harvest storage and in different tissue of the sporophore in *Agaricus bisporus*. Appl Microbiol Biotechnol 70:470–476

Swamy BM, Vikram P, Dixit S, Ahmed HU, Kumar A (2011) Meta-analysis of grain yield QTL identified during agricultural drought in grasses showed consensus. BMC Genomics, 12:319

Szeto YY, Leung GS, Kwan HS (2007) *Le.MAPK* and its interacting partner, *Le.DRMIP*, in fruiting body development in *Lentinula edodes*. Gene 393:87–93

Tachibana S, Oka M (1981) Occurrence of a vitamin B_2-aldehydeforming enzyme in *Schizophyllum commune*. J Biol Chem 256:6682–6685

Van Ooijen JW, Voorrips RE (2001) JoinMap 3.0 software for the calculation of genetic linkage maps. Plant Research International, Wageningen, The Netherlands

Varshney RK, Thudi M, Nayak SN, Gaur PM, Kashiwagi J, Krishnamurthy L, Jaganathan D, Koppolu J, Bohra A, Tripathi S, Rathore A, Jukanti AK, Jayalakshmi V, Vemula A, Singh SJ, Yasin M, Sheshshayee MS, Viswanatha KP (2014) Genetic dissection of drought tolerance in chickpea (*Cicer arietinum* L.). Theor Appl Genet 127:445–462

Voorrips RE (2002) MapChart: software for the graphical presentation of linkage maps and QTLs. J Hered 93:77–78

Wang S, Bastern CJ, Zeng ZB (2012) Windows QTL Cartographer 2.5. Department of Statistics, North Carolina State University, Raleigh, NC. (http://statgen.ncsu.edu/qtlcart/WQTLCart.htm)

Zeng Z (1994) Precision mapping of quantitative trait loci. Genetics 136: 1457–1468